Ultrasound in Med. & Biol., Vol. 00, No. 00, pp. 1–17, 2019

0301-5629/$ - see front matter

https://doi.org/10.1016/j.ultrasmedbio.2019.12.008

● *Original Contribution*

# THREE DECADES OF ULTRASOUND CONTRAST AGENTS: A REVIEW OF THE PAST, PRESENT AND FUTURE IMPROVEMENTS

PETER FRINKING,* TIM SEGERS,† YING LUAN,‡ and FRANÇOIS TRANQUART‡

* Tide Microfluidics, Capitool 41, Enschede, The Netherlands; † Physics of Fluids group, University of Twente, Enschede, The Netherlands; and ‡ R&D Pharmaceutical Diagnostics, General Electric Healthcare, Amersham, UK

(*Received* 24 *July* 2019; *revised* 5 *December* 2019; *in final from* 6 *December* 2019)

**Abstract—Initial reports from the 1960s describing the observations of ultrasound contrast enhancement by tiny gaseous bubbles during echocardiographic examinations prompted the development of the first ultrasound contrast agent in the 1980s. Current commercial contrast agents for echography, such as Definity, Optison, Sonazoid and SonoVue, have proven to be successful in a variety of on- and off-label clinical indications. Whereas contrast-specific technology has seen dramatic progress after the introduction of the first approved agents in the 1990s, successful clinical translation of new developments has been limited during the same period, while understanding of microbubble physical, chemical and biologic behavior has improved substantially. It is expected that for a successful development of future opportunities, such as ultrasound molecular imaging and therapeutic applications using microbubbles, new creative developments in microbubble engineering and production dedicated to further optimizing microbubble performance are required, and that they cannot rely on bubble technology developed more than 3 decades ago. (E-mail: p.frinking@tidemicrofluidics.com)** 

***Key Words:*** **Ultrasound, Contrast agents, Definity, Optison, Sonazoid, SonoVue, Monodisperse, Microbubbles.**

## INTRODUCTION: A REVIEW OF THE PAST

### *A Cloud of Echoes*

The diagnostic applications of ultrasound imaging have been expanded enormously during the last few decades. With the introduction of ultrasound contrast agents (UCA), new meaningful physiologic and pathologic information is provided, and perfusion imaging of myocardial or tumor tissue has now become available for routine clinical decision making. The first observations of the ultrasonic contrast effect date from the mid-1960s to work by Joyner (Gramiak and Shah 1968). Indeed, contrast echocardiography started when it was noted by Gramiak et al. (1969) that the intracardiac injection of indocyanine green dye, a frequently used substance for measuring blood flow, produced a "cloud of echoes" on the M-mode echocardiogram (Gramiak and Shah 1968). In fact, it was shown that the injection of almost any liquid through a small-bore needle or catheter would produce this contrast effect (Kremkau et al. 1968; Kremkau et al. 1970).

Address correspondence to: Peter Frinking, Tide Microfluidics, Capitool 41, Enschede, The Netherlands. E-mail: p.frinking@tidemicrofluidics.com

The effect was referred to as a cloud of echoes although investigators speculated that the phenomenon was owing to the presence of tiny gas bubbles suspended in the liquid (Bove et al. 1968; Ziskin et al. 1972; Barrera et al. 1978). Nevertheless, this correct hypothesis was still challenged, and others suggested that particulate matter caused the ultrasound contrast (Schuchman et al. 1975). Metlzer et al. (1980) provided evidence on this subject and demonstrated, by examining fluids before and after hand agitation employing two syringes connected by a three-way stopcock, that the microbubbles used for peripheral contrast echocardiography were formed during this agitation and thus were already present in the injectant rather than being formed at the catheter tip during injection.

Although free gas bubbles could be generated in any liquid, it was observed that in indocyanine green dye and gelatin microbubble persistence increased, improving contrast enhancement (Meltzer et al. 1980; Carroll et al. 1980). It was concluded that these liquids act as surfactants, decreasing the surface tension to values lower than that of a clean saline-air interface, thereby stabilizing the free gas bubbles against rapid dissolution. Moreover, the surfactants prevented bubbles from

coalescing, minimizing the creation of large and potentially dangerous bubble sizes (Metlzer et al. 1980). Nevertheless, free gas bubbles produced by hand agitation of saline are sometimes still being used in echocardiography for detecting intracardiac shunts.

In the period between 1970−1980, the field of contrast echography evolved further and mainly focused on a wide variety of applications in cardiology such as identification of cardiac structures and cavity dimensions (Roelandt 1982), detection of intracardiac shunts (Valdes-Cruz and Sahn 1984), visualization of blood flow in M-mode, detection of valvular regurgitation (Kerber et al. 1974; Reid et al. 1983), analysis of complex congenital heart disease and cardiac output determination by indicator dilution curves (Meltzer and Roelandt 1982). However, the full potential of contrast echography could still not be explored because of inherent shortcomings of free gaseous microbubbles, such as very short lifetime and low persistence, indeterminate size and inability to pass through the lung circulation after an intravenous injection. Nevertheless, the expectation and confidence in this new modality was very strong, as is illustrated by the following passage from *Contrast Echocardiography* edited by Meltzer and Roelandt (1982):

The future of contrast echocardiography is almost unlimited. As this book indicates, there is a vast amount of interest and research currently being done with regards to contrast echocardiography. Probably the most exciting aspect of this research is the development of new contrast producing agents. It is going to be exciting to see how these various agents develop. Hopefully, one or more of these new agents will be able to traverse the capillaries so that one can visualize the left side of the heart with a peripheral venous injection.

This passage also illustrates the awareness of the limitations at that time, and it took more than a decade to develop the first commercial contrast agent for imaging the left ventricle (LV) of the heart.

*Development of the "ideal" UCA*

From 1980, extensive research was performed in order to make contrast echocardiography an established diagnostic technique (Senior et al. 2017). In 1989, Ophir and Parker (1989) summarized the use of UCA in medical imaging. Five types of agents with different physical properties were classified: free gas bubbles, encapsulated gas bubbles, colloidal suspensions, emulsions and aqueous solutions. In those days, it was still a main challenge to produce the "ideal" contrast agent, which would meet the following criteria:

- Distribution of the agent within the heart chamber or myocardium representative of local blood flow;
- Stability of the agent to persist during an imaging examination after an intravenous injection;
- Consisting of microbubbles smaller than 8 μm in diameter (smaller than red blood cells) enabling passage through the pulmonary system and the smallest capillaries of the body;
- Physiologically inert, excellent safety profile;
- Echogenic, strong and controlled acoustic interaction.

*Stabilized microbubbles*

The challenge of producing stable encapsulated microbubbles surviving passage through the heart and the pulmonary capillary network was first resolved in 1984 (Feinstein et al. 1984), when microbubbles were produced by cavitation after introducing the tip of a sonicator horn into a solution of human serum albumin. These microbubbles could be visualized in the left heart after a peripheral venous injection. During the 1990s, research on gaseous microbubbles as an UCA became very active, and numerous manufacturers started to develop new microbubble-based contrast agents that met most of the criteria listed above. Several technologies for stabilizing the microbubbles were investigated. Thin shells made of protein, polymer or phospholipids were used to reduce surface tension and stabilize the gas core against rapid dissolution. However, the first-generation agents still suffered from limited stability and very short circulation time because of the high solubility of air in water. Persistence during circulation was dramatically improved by replacing air by perfluorinated gases with a low solubility in water, such as sulphur hexafluoride (Schneider et al. 1995), perfluoropropane (Unger et al. 1994) or perfluorobutane (Schneider et al. 1997; Schneider et al. 2011), resulting in a persistence of the agent in the blood circulation sufficient for clinical use. At the end of the decade, more than 15 different agents were at various stages of development. Table 1 summarizes a non-exhaustive list of agents in development for intravenous application at that time (Kasparzak and Ten Cate 1998; Becher and Burns 2000; Stride and Saffari 2003; Quaia 2005; Faez et al. 2013; Chang 2018).

The introduction of the first microbubbles satisfying most criteria required for an intravenous UCA also prompted tremendous research efforts by clinicians, scientists and ultrasound equipment manufacturers to describe the physical phenomena and to translate the knowledge into clinical applications. For example, theoretical expressions for cavitation (Atchley and Crum 1988), the mechanism used for describing the cloud of echoes observed in the beginning on M-mode echocardiograms, proved to be very useful for understanding the interaction between ultrasound waves and gaseous microbubbles. Particularly, the high compressibility of the gas core appearde to be

Table 1. Microbubble-based ultrasound contrast agents for intravenous injection that reached different stages of development during the period between 1990 and 2000.

| Trademark name | Code name | Manufacturer | Formulations: shell/filling gas |
|---|---|---|---|
| Albunex | | Mallinckrodt Pharmaceuticals | Human albumin/air |
| Bisphere | PB127 | Point Biomedical | Polymer bilayer−albumin/air |
| Definity/Luminity | MRX-115/DMP-115 | Bristol-Myers Squibb | Phospholipids/perfluoropropane |
| Echogen | QW3600 | Sonus Pharmaceuticals | Surfactant/dodecafluoropentane |
| Echovist | SH U454 | Schering AG | Galactose/air |
| Filmix | | Cavcon | Lipid/air |
| Imavist (Imagent) | AFO150 (AFO145) | Imcor (Alliance) Pharmaceuticals | Phospholipids/perfluorohexane-air |
| Levovist | SH U508 A | Schering AG | Galactose-palmitic acid/air |
| Myomap | AIP 201 | Quadrant Healthcare | Recombinant albumin/air |
| Optison | FS069 | Amersham Health Inc. | Protein-type A/perfluoropropane |
| Quantison | AIP101 | Quadrant Healthcare | Recombinant albumin/air |
| Sonavist | SH U563 A | Schering AG | Polymer/air |
| Sonazoid | NC100100 | Amersham Health Inc. | Lipid/perfluorobutane |
| SonoGen | QW7437 | Sonus Pharmaceuticals | Surfactant/dodecafluoropentane |
| SonoVue/Lumason | BR1 | Bracco Imaging S.p.A., | Phospholipids/sulphur hexafluoride |
| | AI-700 | Acusphere Inc. | Polymer/perflourobutane |
| | BR14 | Bracco Diagnostics Inc. | Phospholipids/perfluorobutane |
| | BR38 | Bracco Diagnostics Inc. | Phospholipids/perfluorobutane-nitrogen |

Adapted from Kasparzak 1998; Becher and Burns 2000; Stride and Saffari 2003; Quaia 2005; Faez et al. 2013; Chang 2018.

important, since it results in frequency-dependent volume pulsations with a pronounced maximum at the resonance frequency, with the resonance frequency being inversely proportional to the microbubble size (Minnaert 1933; Medwin 1977). Fortunately, the range of microbubble sizes appropriate for clinical use have resonance frequencies on the order of 1−15 MHz, right in the frequency range commonly used in diagnostic ultrasound (Mulvana et al. 2017). Moreover, a resonating bubble behaves as a source of sound rather than as a passive scatterer, yielding an enhancement of particularly non-linear echo signals.

*Non-linear microbubble behavior*

The non-linear echoes produced by gaseous microbubbles stem from intrinsic non-linearities in the Rayleigh-Plesset equation. However, for stabilized microbubbles, the presence of the encapsulating shell substantially affects the volumetric microbubble oscillation amplitude, and the viscoelastic properties of the shell strongly alter its resonance behavior. It has been observed that because of the presence of the shell, encapsulated gas bubbles can be up to 20 times more rigid than free gas bubbles, substantially increasing the resonance frequency. Moreover, because of shell viscosity, bubble oscillations are heavily damped, attenuating the propagating ultrasound wave and thus limiting acoustic penetration depth (de Jong and Hoff 1993; Church 1995; Sontum et al. 1999; Hoff et al. 2000; Sarkar et al. 2005). Since early- to mid-2000, Rayleigh-Plesset−type models including non-linear shell elasticity and viscosity terms were developed (Marmottant et al. 2005; Stride 2008; Tsiglifis and Pelekasis 2008; Paul et al. 2010; Katiyar and Sarkar 2011), predicting the non-linear dynamics of an oscillating microbubble particularly owing to the presence of the stabilizing shell. Excellent reviews on contrast agent modelling are given by Doinikov and Bouakaz (2011) and Faez et al. (2013).

The non-linear dynamics of stabilized oscillating microbubbles includes "compression only behavior," an asymmetric oscillation where a microbubble compresses more than it expands, which was observed experimentally by de Jong et al. (2007) using high-speed imaging. Compression-only results from the non-linear surface tension of an encapsulated microbubble with an equilibrium surface tension close to zero. During compression, the microbubble reaches the tensionless buckling state, whereas volumetric expansions are counteracted by the finite shell elasticity once the bubble reaches the elastic state (Marmottant 2005, Marmottant et al. 2011). Another observation resulting from shell non-linearity, initially described as thresholding (Emmer et al. 2007), appeared to be related to a downshift in the resonance frequency with increasing acoustic pressure at low amplitudes (Overvelde et al. 2010). Others related this behavior to strain softening of the shell (Tsiglifis and Pelekasis 2008; Paul et al. 2010). In fact, the downshift in resonance frequency results from an effective averaging of the shell stiffness over elastic and non-elastic regions, where the elastic region is limited to a relatively narrow microbubble surface area range around the equilibrium bubble area. Thus, the non-linear response of encapsulated microbubbles already appears at very low acoustic pressure amplitudes (*e.g.,* lower than 50 kPa). Higher acoustic pressure amplitudes can result in microbubble destruction and fragmentation. When higher acoustic pressures are applied (*e.g.,* 100−150 kPa for soft-shelled microbubbles and higher than 300 kPa for hard-shelled microbubbles), the shell ruptures transiently and releases free gas bubbles (Frinking et al. 1999), which can rapidly dissolve in the surrounding

liquid. This can generate an abrupt increase of the non-linear harmonics in the backscattered signal, which is a very sensitive way for detecting microbubbles during contrast-enhanced imaging.

*Contrast-specific imaging techniques*

In parallel with the developments of UCA, and because of the improved understanding of non-linear microbubble behavior, specific microbubble imaging modes were developed, and these are currently implemented in most clinical ultrasound systems (Burns et al. 1996; Wei et al. 1998; Hope Simpson et al. 1999). The contrast-specific imaging modes take advantage of non-linear acoustic properties of gas bubbles very different from those of tissue (Frinking et al. 2000; Rafter et al. 2004). Particularly, the non-linear shell behavior explains the success of low mechanical index (MI) (<0.1) contrast-specific imaging mostly used for real-time perfusion and intra-cavitary assessments. Additionally, several diagnostic imaging techniques and/or quantification methods (*e.g.,* harmonic power Doppler, destruction-replenishment imaging) are based on the unique and very sensitive property of microbubble destruction when short pulse excitations at higher MI are applied (Blomley et al. 1999; Albrecht et al. 2003). Integration of these bubble-specific signatures in combination with excellent tissue suppression algorithms in imaging systems resulted eventually in broad clinical acceptance of contrast-enhanced ultrasound imaging as a diagnostic mode, particularly outside cardiology, with equivalent or even superior clinical performance compared with other contrast-enhanced modalities such as magnetic resonance imaging (MRI) and computed tomography (CT) (Lu et al. 2007; Meloni et al. 2008; Sidhu et al. 2018).

## THE PRESENT: COMMERCIALLY AVAILABLE CONTRAST AGENTS

Most of the agents initially developed for intravenous use are listed in Table 1, and from those reaching clinical approval during the last 3 decades (Table 2), only four are currently marketed and used in routine clinical practice. Three of these agents are phospholipid-shelled agents (SonoVue, Definity, Sonazoid) and one is an albumin-shelled agent (Optison). The formulations, physico-chemical properties, clinical applications and new development of these agents are described in further detail below and summarized in Tables 3 and 4.

*Optison*

Optison (perflutren protein-type A microspheres injectable suspension) (USP, GE Healthcare, AS, Oslo, Norway) is a sterile non-pyrogenic suspension consisting of microspheres with a perflutren (Octafluoropropane) gas core encapsulated by a 15 nm thick human serum albumin

Table 2. Clinically approved ultrasound contrast agents.

| Name | First approved for clinical use | Shell material | Gas | Application (examples) | Producer/distributor | Countries |
|---|---|---|---|---|---|---|
| Optison | 1998 | Cross-linked serum albumin | Octafluoropropane | Left ventricular opacification, endocardial border delineation, Doppler | GE healthcare, Buckinghamshire, UK | USA, Europe |
| Sonazoid | 2006 | Hydrogenated egg yolk phosphatidyl serine (HEPS) | Perfluorobutane | Myocardial perfusion, liver imaging | GE healthcare, Buckinghamshire, UK/ Daiichi Sankyo, Tokyo, Japan | Japan, South Korea, Norway, Taiwan, China |
| Lumason/SonoVue | 2001/2014 | Phospholipid | Sulphur hexafluoride | Left ventricular opacification, microvascular enhancement (liver and breast lesion detection) | Bracco Diagnostics Inc., Monroe Township, NJ, USA/Bracco Imaging S.p.A., Colleretto Giacosa, Italy | USA, Europe, China, Brazil |
| Definity/Luminity | 2001/2006 | Phospholipid | Octafluoropropane | Echocardiography, liver/kidney imaging (Canada) | Lantheus Medical Imaging Inc, North Billerica, MA, USA | North America, Europe |
| Imagent/Imavist | 2002, withdrawn | Phospholipid | Perfluorohexane, Nitrogen | Echocardiography, heart perfusion, tumor/blood flow anomalies | Schering AG, Berlin, DE | USA |
| Echovist | 1991, withdrawn | Galactose microparticles | Air | Right heart imaging | Schering AG, Berlin, DE | Germany, UK |
| Levovist | 1995, withdrawn | Galactose microparticles, palmitic acid | Air | Whole heart imaging, Doppler imaging | Schering AG, Berlin, DE | Canada, Europe, China, Japan |
| Albunex | 1993, withdrawn | Sonicated serum albumin | Air | Transpulmonary imaging | Molecular Biosystems Inc., San Diego, CA, USA | Japan, USA |

Adapted from Paefgen et al. 2015.

Table 3. Clinical ultrasound contrast agents currently commercially available.

| | SonoVue/Lumason | Definity/Luminity | Optison | Sonazoid |
|---|---|---|---|---|
| Manufacturer | Bracco Imaging S.p.A. | Lantheus Medical Imaging Inc | GE Healthcare | GE healthcare/Daiichi Sankyo |
| Approval indication(s) | LVO/EBD, breast,* liver,* vascular,* urinary tract | LVO/EBD, breast,* liver,* vascular* | LVO/EBD | Myocardial perfusion,* liver,* breast* |
| Countries available | North America, Europe, Brazil, Asia | North America, Europe, Australia, Asia | North America, Europe | Japan, South Korea, Norway, Taiwan, China |
| Shell/gas | Phospholipid/sulphur hexafluoride | Phospholipid/perflutren | Albumin/perflutren | Phospholipid/ perfluorobutane |
| Contraindications | Hypersensitivity to sulphur hexafluoride or any inactive ingredient | Hypersensitivity to perflutren | Hypersensitivity to perflutren, blood, blood products or albumin | Egg allergy |
| Vial supplied | 10 mL, vial containing 25 mg powder 5 mL saline | 2 mL vials | 3 mL vials | 16 $\mu$l of perflubutane microbubbles in one vial<br>2 mL sterile water for injection |
| Storage | Room temperature | 2−8˚C | 2−8˚C | Below 25˚C |
| Typical doses | 2 mL of reconstituted agent | Weight based bolus (10 μL/kg) or infusion rate of 4.0 mL/min of 1.3 + 50 mL saline | 0.5 mL | Weight based 15 μL/kg or 0.12 μL MB/kg |
| Administration recommendation | Bolus<br>Bolus dose can be repeated once<br>Doses varies depending on age and indication | Bolus or infusion<br>Dose varies based on organ being imaged | Rate not exceed 1 mL/s<br>Max dose in 10 min: 5 mL<br>Max dose for one study: 8.7 mL | Bolus or infusion |
| MI | MI ≤ 0.8 | MI ≤ 0.8 | Safety of MI >0.8 has not been tested | MI ≤0.8 |
| Advantages | Approved for use in pediatric populations<br>Reconstitution by hand mixing | Bolus or infusion | Resuspend by hand mixing | Bolus or infusion |
| Notes | Bolus and infusion dosing are used, although package insert only describes bolus dosing | Requires 45-s activation on VialMix. Hand agitation thereafter if being used >5 min after activation | Bolus and infusion dosing are used | Re-injection can be used for Kupffer phase imaging |

EBD = endocardial border definition; LVO = left ventricular opacification; MB = microbubble; MI = mechanical index.
* Only in certain countries.Adapted from Chang 2018.

Table 4. Size distribution characteristics from the commercially available agents.

| Products | DN (μm) | DV50 (μm) | Conc.T. ($\times 10^8$ MB/mL) | MB >10 μm ($\times 10^8$ MB/mL) | MVC (μL/mL) |
|---|---|---|---|---|---|
| SonoVue | 1.92 ± 0.09 | 8.01 ± 0.85 | 3.4 ± 0.5 | 0.022 ± 0.006 | 6.5 ± 1.2 |
| Definity | 1.22 ± 0.03 | 8.19 ± 0.77 | 84.0 ± 11.1 | 0.143 ± 0.042 | 44.0 ± 9.5 |
| Optison | 3.08 ± 0.04 | 7.11 ± 0.24 | 7.3 ± 0.2 | 0.078 ± 0.017 | 35.2 ± 3.0 |
| Sonazoid | 2.1 ± 0.1 | 2.6 ± 0.1 | 12 ± 0.1 | - | 8.0 ± 0.6 |

DN indicates diameter in number; DV50, diameter in volume; Conc.T., total concentration; MB, microbubbles; MVC, microbubble volume concentration. Adapted from Hyvelin et al. 2017.

shell (Optison package insert 2018). The reconstitution of Optison is by gentle hand mixing, and the concentration of the reconstituted suspension is $5.0-8.0 \times 10^8$ microspheres/mL with an average diameter of 3.0−4.5 μm, and 95% of microspheres are smaller than 10 μm.

The acoustical characteristics of Optison were investigated previously, and both mathematical modelling and experimental measurements were utilized (Church 1995; Podell et al. 1999; Bing et al. 2018). The albumin shell rigidity of 88.8 MPa and a shell shear viscosity of 0.177 N s/m$^2$ were derived, by assuming the shell as a continuous surface layer of incompressible solid elastic material and by accounting for damping provided by the shell viscosity. Based on data for Albunex (de Jong and Hoff 1993), the air-based predecessor of Optison, values for shell elasticity and dilational viscosity can be estimated as 4 N/m and $3.2 \times 10^{-8}$ kg/s, respectively (Morgan et al. 2000; Forbes and O'Brien 2012). *In vitro* measurements indicated that the destruction (or gas dissolution) pressure threshold for rapid destruction of Optison was 0.47 MPa (peak-negative pressure) when exposed to 3.5-MHz ultrasound (Podell et al. 1999), while a lower threshold was found to contribute to accelerated dissolution (Porter et al. 2006). The flexible and robust characteristics of the albumin shell make Optison an effective ultrasound scatterer, while it can be resilient to destruction in clinical use.

Optison was launched as the first of the second-generation of UCA in the North American market in January 1998 and in Europe in May of the same year (Jackson et al. 2016). It is indicated for use in patients with suboptimal echocardiograms to opacify the LV and to improve the delineation of left ventricular endocardial borders (Fig. 1). Off-label use of Optison was reported, including stress echocardiography of patients with suboptimal baseline echocardiograms (Dolan et al. 2001, 2009; Dawson et al. 2009), as well as its non-cardiac clinical applications in liver imaging (*i.e.,* for monitoring the evolving necrosis during thermoablation of liver tumors [Jung et al. 2003]), and it was reported in pediatric patients, such as for the assessment of solid pediatric tumors (McCarville et al. 2012) and detection of vesicoureteral reflux (VUR) in children (Ntoulia et al. 2018).

During clinical imaging, Optison can be administered intravenously as either a bolus (0.3−0.5 mL) with a slow rate (not exceeding 1 mL/s) or continuous infusion (10% dilution, 3−5 mL/min). This should be followed by 5−10 mL saline flushes over 10 s to avoid acoustic shadowing and permit steady-state concentration of microbubbles during image acquisition. The recommended Optison dose is 0.5−3.0 mL per patient, with the duration of the left-ventricular contrast of 2.5−4.5 min. A low MI (MI lower than 0.2) in clinical imaging is recommended to avoid microbubble destruction (Porter et al. 2018).

*Definity*

Definity (USA) or Luminity (EU) (perflutren lipid microspheres) (Lantheus Medical Imaging Inc, North Billerica, MA, USA) injectable suspension is supplied as a single-use 2 mL glass vial containing a clear liquid and octafluoropropane ($C_3F_8$) gas in the head space. The liquid contains a solution with the three phospholipids DPPC (1,2-Dipalmitoyl-sn-glycero-3-phosphocholine), DPPA (1,2-Dipalmitoyl-sn-glycero-3-phosphate, sodium salt) and DPPE-MPEG5000. The product is prepared by emulsification activation using a mechanical shaking device (Vialmix) Lantheus Medical Imaging Inc, North Billerica, MA, USA) for 45 s. After activation, a 1 mL milky-white liquid suspension is obtained containing $84.0 \pm 11.1 \times 10^8$ microspheres/mL (44.0 μL/mL volume concentration) with the number mean diameter of 1.22 ± 0.03 μm and volume median diameter of 8.19 ± 0.77 μm (Hyvelin et al. 2017). The viscoelastic shell properties for Definity microbubbles have been estimated at high (12−29 MHz) and at low (5−15 MHz) ultrasound frequencies (Goertz et al. 2007, Faez et al. 2011). At the lower frequencies, values corresponding to 0.82 N/m for the shell elasticity and $4.0 \times 10^{-9}$ kg/s for dilational viscosity have been reported (Faez et al. 2011), which are significantly lower compared with those mentioned above for Optison.

Definity is one of the second-generation microbubble contrast agents approved for left ventricular opacification and left ventricular endocardial border detection. It was approved in July 2001 by U.S. Food and Drug Administration (FDA) (Definity drug approval package) and in September 2006 by the European Medicine Agency under the name Luminity (European Public Assessment Report [EPAR] summary for the public).

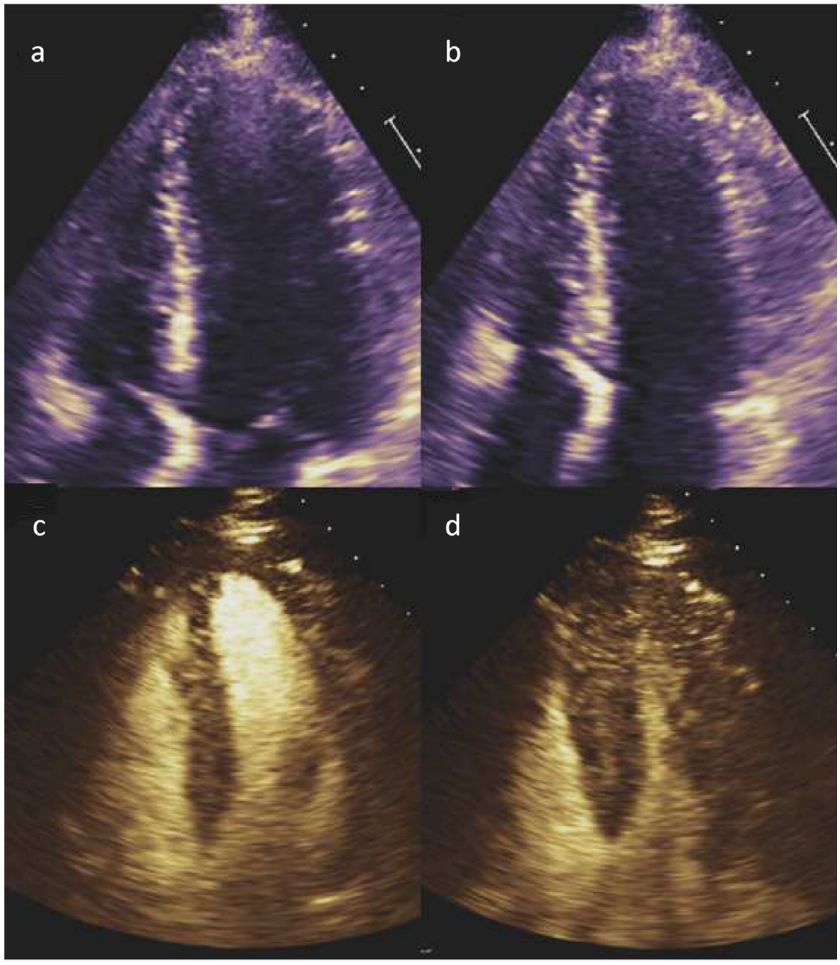


Fig. 1. Representative pre-contrast images of a patient who had minimal endocardium visualized on the four chamber view and complete visualization after Optison contrast enhancement: (a) Diastole before contrast. (b) Systole before contrast. (c) Diastole after contrast. (d) Systole after contrast. From Zhao et al. 2017.

The pharmacokinetics of an intravenous dose of activated Definity was evaluated in healthy humans and those with chronic obstructive pulmonary disease. The perflutren gas is cleared by the lungs in the expired air in an unchanged state. The rapid elimination of perflutren gas in the expired air was also consistent with the rapid disappearance of ultrasound contrast enhancement after activated Definity administration (Abdelmoneim and Mulvagh 2012).

Beyond enhanced endocardial visualization, Definity is used for quantification of LV volumes and ejection fraction (Mulvagh et al. 2008). Moreover, the diagnoses of apical LV pathology (*e.g.,* apical variant of hypertrophic cardiomyopathy and thrombus), post−myocardial infarction complications (*e.g.,* LV rupture or pseudoaneurysm, or ventricular septal defect) and intracardiac masses (Porter et al. 2014) are significantly enhanced (Fig. 2). In addition to its cardiac indications, Definity is also approved for imaging of the liver and kidney in Canada and Australia. Several studies have shown its efficacy in evaluation of liver lesions as a vascular phase agent (Claudon et al. 2013).

As mentioned by Abdelmoneim and Mulvagh (2012), off-label use of Definity has been reported for the use with stress echocardiography improving the diagnostic accuracy of stress echo in the diagnosis of coronary artery disease (Moir et al. 2004; Tsutsui et al. 2005; Plana et al. 2008; Dolan et al. 2009) primarily to identify wall motion abnormalities in clinically indicated stress echo studies. Moreover, a growing number of published articles have documented the use of Definity for the assessment of myocardial perfusion to detect perfusion abnormalities both at rest and in conjunction with exercise and pharmacologic stress echocardiography (Abdelmoneim et al. 2009a, 2009b).

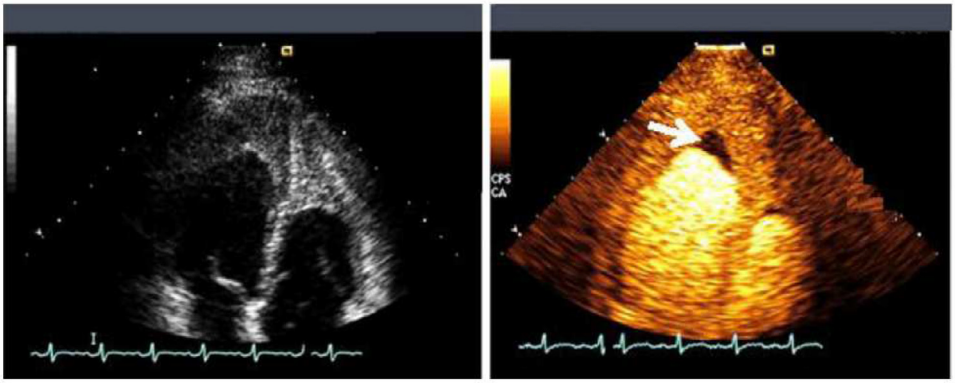

Fig. 2. Unenhanced (*left*) and real-time very low MI Definity contrast-enhanced (*right*) images of a patient with an apical mass. Real-time very low MI contrast-enhanced imaging delineates perfused and non-perfused areas due to endomyocardial fibrosis with thrombus formation (*arrow*). From Porter et al. 2014. MI = mechanical index.

*SonoVue*

SonoVue (sulphur hexafluoride [$SF_6$] microbubbles) (Bracco Imaging S.p.A., Colleretto Giacosa, Italy) or Lumason (sulphur hexafluoride lipid-type A microspheres) (Bracco Diagnostics Inc., Monroe Township, NJ, USA), is supplied as a kit containing a single-use septum-sealed vial of phospholipid lyophilized powder and $SF_6$ headspace, a pre-filled syringe with 5 mL sodium chloride 0.9% injection (diluent) and a mini-spike transfer system (Hyvelin et al. 2017). The lyophilizate consists of polyethylene glycol 4000 and phospholipids DSPC (1,2-Distearoyl-sn-glycero-3-phosphocholine) and DPPG (1,2-Dipalmitoyl-sn-glycero-3-phosphoglycerol, sodium salt) (Schneider et al. 1995). The product is prepared by reconstitution of the lyophilized cake and by shaking the vial for 20 s to obtain a homogenous milky-white suspension of microbubbles, which can be stored for up to 6 h. After reconstitution, the product contains approximately $3.4 \pm 0.5 \times 10^8$ microspheres/mL (6.5 μL/mL volume concentration) with the number mean diameter of $1.9 \pm 0.1$ μm and volume median diameter of $8.0 \pm 0.9$ μm (Hyvelin et al. 2017).

SonoVue is mostly administered as intravenous bolus injection followed by a 5−10 mL saline flush and should be gently agitated before administration. The clinical dose recommended for a single injection is 34 μL/kg (*i.e.,* 2.4 mL for a 70 kg person) (Hyvelin et al. 2017); however, the optimal dose may depend on the individual patient and possibly on the scanner technology used. Repeated injection is possible, but in some situations, it is preferred to extend the examination under steady-state conditions (*e.g.,* to prolong the duration of hepatic parenchymal enhancement [Quaia et al. 2016] or for measurement of blood flow parameters for assessment of oncologic response to therapy using the destruction-replenishment technique [Dietrich 2018]). For this, a dedicated infusion pump (Vueject, Bracco Imaging, Milan, Italy) with a rotating syringe holder to avoid decantation of the microbubbles has been developed. In this case, SonoVue can be administered as a continuous infusion at a rate of about 1 mL/min depending on the enhancement level required (Schneider 2002, Greis 2004).

Pharmacokinetics of SonoVue was assessed in humans showing that $SF_6$ is rapidly removed from the blood by the pulmonary route. After intravenous injection, the microbubbles are submitted to systemic pressure variations during the cardiac cycle. The high molecular weight gas $SF_6$, having a low solubility in water and blood, confers good pressure resistance to SonoVue microbubbles (Schneider et al. 1995, Bokor 2000).

Acoustic properties such as attenuation, backscatter and non-linear behavior of SonoVue microbubbles have been extensively studied (Schneider et al. 1995; Gorce et al. 2000; Vandermeer et al. 2004; Biagi et al. 2007; Chetty 2008; Tu 2009). Visco-elastic shell parameter values of 0.55 N/m for the shell elasticity and $7.2 \times 10^{-9}$ kg/s for dilational viscosity have been reported (Gorce et al. 2000, Marmottant et al. 2005), which are very similar to Definity. Moreover, de Jong et al. (2007) reported the extremely non-linear characteristic of compression-only behavior, which was observed during the first high-speed imaging recordings (Chin et al. 2003) and appeared to be a typical characteristic of shelled microbubbles. In fact, these observations motivated the development of the Marmottant model (Marmottant et al. 2005) for phospholipid-shelled microbubble dynamics and enforced the fundamental understanding of the success of low-MI contrast-specific imaging techniques in combination with SonoVue.

SonoVue has clinically been approved in Europe (2001) and China (2004) for use in adult patients with suboptimal echocardiograms to opacify the left ventricular chamber and to improve the delineation of the left ventricular endocardial border, for focal liver lesion and for focal breast lesion characterization (EPAR summary for the public). In 2014, Lumason obtained approval in the United

States for adult patients with suboptimal echocardiograms to opacify the left ventricular chamber and to improve the delineation of the left ventricular endocardial border; in March 2016 it was the first UCA receiving FDA approval for characterizing focal liver lesions in adult and pediatric patients (Lumason drug approval package). Recently, approval for ultrasonography of the urinary tract for the evaluation of suspected or known VUR in pediatric patients was obtained in the United States (2016), Europe (2017) and China (2018). Aside from approved indications, a wide variety of off-label use has been listed primarily for SonoVue in adult (Sidhu et al. 2018) and pediatric patients (Sidhu et al. 2017). Some of the most popular clinical applications of SonoVue are for the diagnosis of focal liver lesions, guidance during ablative treatment and follow-up of liver tumors (Ferraioli and Meloni 2018) (Fig. 3).

*Sonazoid*

Sonazoid microspheres (GE Healthcare, Buckinghamshire, UK; Daiichi Sankyo, Tokyo, Japan) is a second-generation UCA that has been approved in Japan (2006), South Korea (2012), Norway (2014), Taiwan (2017) and mainland China (2018) for contrast-enhanced sonography of focal liver lesions. In Japan, it was approved for contrast-enhanced imaging of breast lesions in 2012.

Sonazoid is formulated as a lyophilized powder for injection that consists of perfluorobutane ($C_4F_{10}$) microspheres stabilized by a monomolecular membrane of hydrogenated egg yolk phosphatidyl serine (HEPS). The product is reconstituted before use with sterile water through a supplied vented filter spike (5 μm) followed by manual mixing for 1 min. After reconstitution, the product appears as a milky white, homogeneous suspension, containing approximately $1.2 \pm 0.1 \times 10^9$ microspheres/mL (8 μL/mL volume concentration) with the number mean diameter of $2.1 \pm 0.1$ μm and volume median diameter of $2.6 \pm 0.1$ μm (Sontum et al. 2008). Characteristic acoustic properties of Sonazoid microbubbles were described by Katiyar and Sarkar (2011) using various models for encapsulated microbubbles. Visco-elastic shell parameter estimations obtained with the Marmottant model (Marmottant et al. 2005) resulted in values of 0.5−0.6 N/m for the shell elasticity and $1.2 \times 10^{-8}$−$1.6 \times 10^{-8}$ kg/s for dilational viscosity (Faez et al. 2011); the dilational viscosity is 2−3 times higher compared to SonoVue and Definity, respectively. Sonazoid is highly resistant to overpressures; pressure stress up to 300 mmHg is well tolerated by both concentrated and diluted suspensions (Sontum 2008). The composition of the suspension, physicochemical properties and visco-elastic properties of the stabilizing membrane showed a low variance from vial to vial and from batch to batch, which ensures the consistency in the biologic behavior and clinical efficacy of Sonazoid (Sontum et al. 1999; Hoff et al. 2000; Sontum 2008).

The pharmacokinetics and clinical assessment of Sonazoid showed a very good tolerance of the recommended clinical dose of 0.12 μL perfluorobutane microbubbles/kg weight in healthy adults (Li et al. 2017). Low MI (around 0.2 depending on the scanners) together with contrast-specific non-linear imaging methods should be used to avoid microbubble destruction. As for any agent, the dosage and scanner settings should be adjusted based on patient's body habitus, tissue attenuation, depth of lesions and specific requirements for repetitive injection.

With clinical imaging of Sonazoid in liver, two phases of contrast enhancement are observed: a vascular phase, followed by a post-vascular phase or Kupffer phase. During Kupffer phase imaging, or parenchyma-specific imaging, the normal hepatic parenchyma is enhanced, and malignant lesions appear as clear contrast defects (Moriyasu and Itoh, 2009). The pattern of vascular phase and Kupffer phase enhancement can be used to better characterize focal liver lesions and to detect or rule out the presence of lesions (Correas et al. 2011; Jo et al. 2017; Zhai et al. 2019).

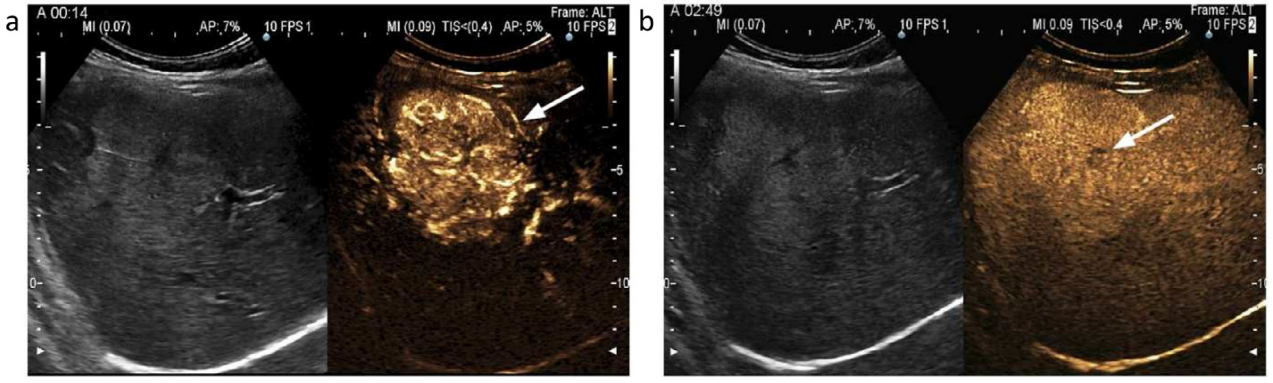


Fig. 3. Focal nodular hyperplasia (FNH) in a 36-y-old woman without a history of liver disease. (a) Spoke-wheel−like enhancement with centrifugal filling in the early arterial phase 15 s after SonoVue injection. (b) In the delayed phase (3 min after injection), the lesion exhibits sustained enhancement except for a central scar (*arrow*). From Ferraioli and Meloni 2018.

Additionally, the prolonged time window during Kupffer phase imaging enables repeated scanning up to 10−60 min after injection, improving lesion detection. Kudo (2016) developed a defect reperfusion imaging method during which the contrast is re-injected based on enhancement defects detected during the stable Kupffer phase, providing additional information on arterial enhancement to improve the accurate diagnostic and treatment strategy of hepatocellular carcinoma. Figure 4 shows exemplary images after Sonozoid injection of liver metastasis and focal nodular hyperplasia (FNH). Off-label use of Sonazoid has been reported such as for the detection of sentinel lymph nodes (Shimazu et al. 2017).

All commercial contrast agents meet the criteria as defined more than 3 decades ago for successful clinical utility after intravenous injections, particularly in terms of demonstrating an excellent safety profile (Main et al. 2007; Claudon et al. 2012). Variations in composition, physico-chemical and shell visco-elastic properties between the agents, as reported above, allows for specific applications depending on the agent. For example, the extremely non-linear behavior of SonoVue and Definity at low MI (lower than 0.1) is exploited (*e.g.,* for real-time imaging in deep tissue where the ultrasound beam can be severely affected by attenuation). On the other hand, Sonazoid's high persistence and resistance to acoustic pressure allows its microbubbles to facilitate a specific Kupffer uptake (Fig. 5) not seen with the other marketed agents (Watanabe et al. 2007; Yanagisawa et al. 2007).

## FUTURE IMPROVEMENT

While contrast-specific detection technology has seen dramatic progress since the introduction of UCA, successful clinical translation of new developments has been limited during the same period, while understanding of microbubble physical, chemical and biologic behavior has improved substantially. Indeed, technology has made enormous advancements with the introduction of, for example, targeted microbubbles for molecular imaging and for therapeutic applications, but none of these developments have resulted in new clinical agents specific to these applications. This section will

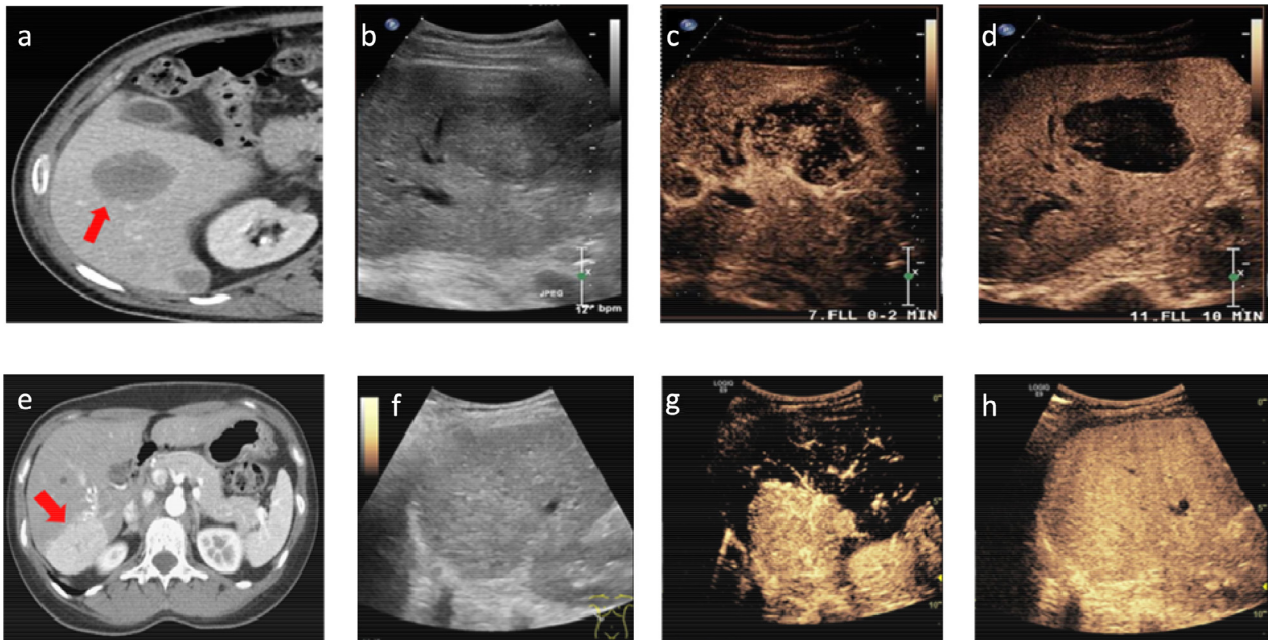


Fig. 4. Sonazoid-enhanced imaging of focal liver lesions. (a−d) A 75-y-old man with liver metastasis; (e−h) A 38-y-old woman with FNH. (a) A CE-CT image displays slight peripheral enhancement with hypoattenuating centre. (b) Pre-contrast harmonic B-mode shows isoechoic metastasis. (c) Arterial phase post−Sonazoid injection shows metastasis with non-enhancing regions. (d) Kupffer phase at 10 min post−Sonazoid injection shows metastasis non-enhancing with well-defined rim. (e) FNH hyperintense representation in the venous/delayed phase on CE-CT. (f) Pre-contrast harmonic B-mode image of FNH. (g) Arterial phase shows well-defined lesion margins and central scarring. (h) Kupffer phase at 10 min post−Sonazoid injection shows homogeneous iso-enhancement of FNH. From: An Efficacy and Safety Study of Sonazoid and SonoVue in Participants With Focal Liver Lesions, Undergoing Pre- and Post-Contrast Ultrasound Imaging (ClinicalTrials.gov Identifier: NCT03335566). This phase 3 prospective study was conducted at 17 centres in greater China and Korea (May 2014 to April 2015). The study was approved by an independent ethics committee or independent review board at each clinical site according to national or local regulations. Written informed consent was obtained from all study participants. CE-CT = contrast-enhanced computed tomography; FNH = focal nodular hyperplasia.

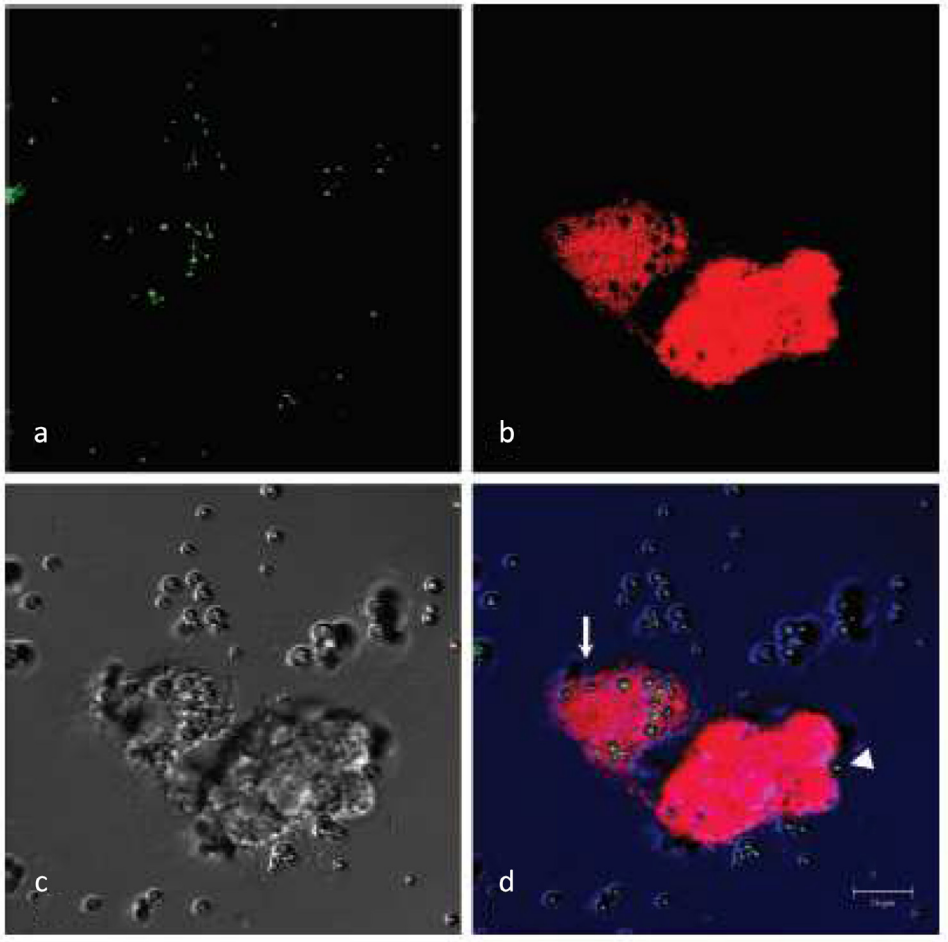


Fig. 5. Confocal laser scanning microscopy (CLSM) and phase-contrast microscopy indicating uptake/phagocytic process of Sonazoid microbubbles by Kupffer cells. (a) Microbubbles detected as reflected light (*green spots*). (b) Stained cytoplasm of Kupffer cells (*red*). (c) Differential interference contrast image. (d) An overlay of panels a, b and c. Strong reflected light spots from Sonazoid microbubbles were observed in the cytoplasm of isolated Kupffer cells. Single microbubble attached to the outside of cell membrane could be discriminated, as it was not surrounded by the cytoplasm (*arrowhead*). From Watanabe et al. 2007.

focus on a new advancement that can be employed to optimize microbubble performance.

*Monodisperse microbubbles*

The production methods of commercially available contrast agents result in microbubble suspensions with inherently polydisperse size distributions, typically ranging from 1−10 μm in diameter (Stride and Saffari, 2003). Microbubbles excited near their resonance frequency exhibit the strongest relative radial excursion and thereby produce the strongest non-linear echo response (Leighton, 1994; Segers et al. 2016a). Clinical ultrasound scanners operate at a narrow frequency bandwidth relative to the resonance frequencies of the microbubbles present in a typical polydisperse UCA. Consequently, only a small fraction of the microbubbles is excited near their resonance frequency and contributes to the generation of the non-linear echo. Indeed, it has frequently been suggested that the sensitivity of contrast-enhanced ultrasound imaging can be improved by narrowing down the microbubble size distribution (Talu et al. 2007; Streeter et al. 2010). In fact, a sensitivity increase of 2−3 orders of magnitude has been measured *in vitro* for resonantly driven monodisperse microbubbles compared with a polydisperse agent (Segers et al. 2018b).

*Monodisperse microbubbles for molecular imaging*

The increased sensitivity provided by monodisperse microbubbles may particularly be of interest in ultrasound molecular imaging applications using ligand-bearing microbubbles, which can be targeted to specific receptors expressed on endothelial cells (Klibanov 2006). Successful binding of

these molecular agents is non-trivial and depends on, for example, ligand-receptor affinity, ligand density, level of receptor expression, vessel diameter and wall shear rate (Tranquart et al. 2014). Although promising pre-clinical results have been reported demonstrating high ligand-receptor affinity and specificity (Pochon et al. 2010; Tardy et al. 2010), clinical translation has not yet resulted in approval of any ultrasound molecular imaging agent, despite positive initial clinical results (Smeenge et al. 2017; Willmann et al. 2017). It has been suggested that this is partially due to the polydisperse character of these agents, resulting in a suboptimal performance even at an agent dose corresponding to approximately 10 times the typical imaging dose used with a non-targeted agent such as SonoVue (Frinking et al. 2012). The suboptimal performance results from the fact that only small fractions of the total injected number of primarily off-resonant microbubbles bind to the target site. Thus, an acoustically uniform and narrowband response of monodisperse microbubbles (Segers et al. 2016b) may dramatically improve imaging sensitivity of individually bound microbubbles. Moreover, monodisperse bubbles may allow for successful discrimination of targeted microbubbles from freely circulating ones through spectral changes owing to a resonance frequency shift of the microbubbles of a given size after binding (Overvelde et al. 2011).

*Monodisperse microbubbles for theragnostic applications*

The narrowband and acoustically uniform response of a monodisperse microbubble suspension is furthermore of great interest for emerging theragnostic applications using microbubbles and ultrasound. The echogenic bubble can be tracked in the body while at increasing acoustic pressures it can locally deliver a drug payload (Tsutsui et al. 2004; Hernot and Klibanov 2008; Deelman et al. 2010; Carson et al. 2012; Dewitte et al. 2015), induce cell poration (Helfield et al. 2016), temporarily open the blood–brain barrier (Hynynen et al. 2006; Choi et al. 2010; Konofagou et al. 2012) or lyse a blood clot (Molina et al. 2009). Key to all these emerging applications is a precise control over the interaction of microbubbles with the ultrasound wave (Stride and Edirisinghe 2009) to induce a maximal therapeutic effect while minimizing possible side effects such as haemorrhage and cell death (Karshafian et al. 2009; Wang et al. 2015; Snipstad et al. 2017). Such an accurate control over volumetric microbubble oscillations can be achieved by using monodisperse microbubbles. Furthermore, because of their uniform acoustic response, monodisperse microbubble populations may potentially solve remaining fundamental questions as to the optimal acoustic parameters and corresponding volumetric oscillation amplitudes required to induce therapeutic effects such as endocytosis, sonoporation and cell death (Karshafian et al. 2009; van Rooij et al. 2016: Roovers et al. 2019).

*Production techniques for monodisperse microbubbles*

For all these reasons, efforts have been made to develop next-generation microbubble agents with a narrow and controllable size distribution. To date, two strategies exist for achieving this. The first approach is based on isolating a subset of sizes from the native size distribution of a polydisperse microbubble suspension. This can be done by mechanical filtration (Emmer et al. 2009) (Fig. 6a), by decantation (Goertz et al. 2007) (Fig. 6b), by centrifugation (Feshitan et al. 2009) (Fig. 6c) or by pinched flow fractionation (Kok et al. 2015) (Fig. 6d). However, size uniformity obtained by these methods does not necessarily result in acoustic uniformity. However, polydisperse agents can also be sorted to their acoustic resonance in an acoustic bubble sorting chip (Segers and Versluis 2014) (Fig. 6e). It has been shown that an acoustically sorted bubble suspension has a uniform acoustic response (Segers et al. 2016a). A further limitation of the aforementioned sorting methods is that typical native size distributions of polydisperse agents primarily consist of small bubbles (smaller than 2–3 μm in diameter), whereas it has been suggested that larger bubbles (approximately 4–5 μm in diameter) are preferable for therapeutic applications such as blood–brain barrier opening, since these bubbles are resonant to ultrasound frequencies typically used for therapy (lower than 1 MHz) (Choi et al. 2010).

The second approach for producing monodisperse microbubbles is through direct bubble formation in a microfluidic flow-focusing device (Ganan-Calvo and Gordillo 2001; Anna et al. 2003; Garstecki et al. 2004; Garstecki et al. 2005; Dollet et al. 2008). In such a device, a gas thread is focused between two liquid flows through a constriction where it destabilizes because of capillary instability and pinches off to release monodisperse bubbles (Fig. 6f). The bubble size, stability and the generation frequency can now be accurately controlled through the gas pressure, the liquid flow rate and the lipid mixture (Segers et al. 2016b, 2017, 2019). Bubble formation rates exceeding 1 million bubbles per second can be achieved using a single nozzle (Castro-Hernandez et al. 2011; Segers et al. 2016b), and 2.4 mL of a monodisperse microbubble suspension can be produced in 15 min using a microfluidic device as shown in Figure 6f. This would translate into producing a clinically relevant imaging dose in less than 1 min, considering the 2–3 orders of magnitude gain in sensitivity for monodisperse microbubbles compared with SonoVue (Segers et al. 2018b, 2019).

The acoustic response of monodisperse microbubble suspensions was shown to have a narrowband and uniform response (Segers et al. 2016a, 2016b, 2018).

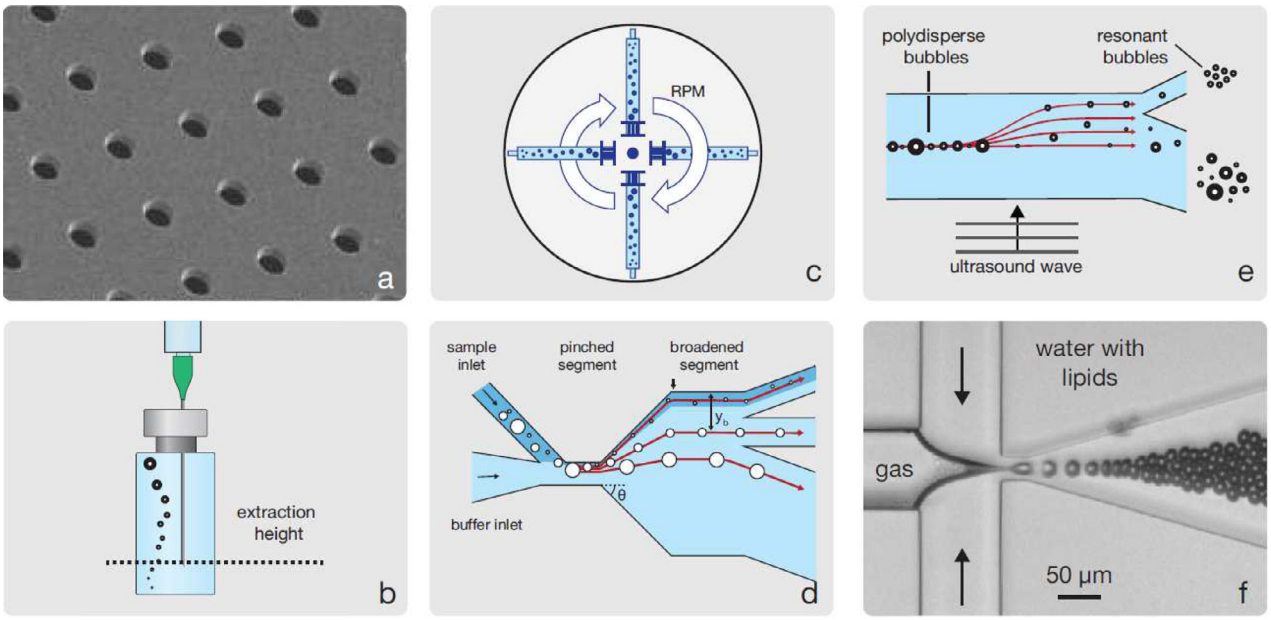


Fig. 6. Different strategies to produce microbubbles with a narrow size distribution. (a) Pore filters can be used to filter bubbles to size (Emmer et al. 2009). Bubbles can be sorted using the volume-dependent gravitational force, either directly by (b) decantation or through (c) centrifugation. (d) Pinched flow fractionation is a microfluidic sorting technique. The microbubbles are pinned to the top wall of the pinched segment by a co-flow. Size-selective sorting is achieved through expansion of the pinched segment into the broadened segment. (e) Acoustic bubble sorting sorts bubbles to their acoustic resonance behavior rather than to their size using the primary acoustic radiation induced by a traveling acoustic wave. (f) Microbubbles can be directly synthesized in a flow-focusing device. Figure is based on Segers et al. (2014, 2018a). Figure 6a was taken from Aquamarijn, The Netherlands (from https://www.aquamarijn.nl/technology/ with permission).

However, to date, questions remain as to the exact clinical requirements regarding monodispersity in terms of size and acoustic resonance behavior for imaging and especially for therapeutic applications. It is, for example, being debated that the improved sensitivity observed with monodisperse microbubbles may also be obtained with a polydisperse agent by injecting a higher dose (Talu et al. 2007; Kaya et al. 2010). Future studies are thus required to investigate the full clinical potential and *in vivo* performance of monodisperse microbubbles. Nevertheless, the current advances look promising, and these can drive forward emerging applications of lipid-coated microbubbles in combination with ultrasound that are currently suboptimal owing to the use of polydisperse agents.

## CONCLUSION

Contrast-enhanced ultrasound imaging has seen tremendous progress during the last 3 decades. Historically, the clinical focus was primarily on echocardiography, for which LV opacification (i.e., improving LV endocardial border delineation) was the major indication, while myocardial perfusion was described as the holy grail and considered as a major market for contrast echo. The commercial agents have proven to be successful; however, there is still no approval for myocardial perfusion, and major clinical applications of contrast-enhanced ultrasound are outside cardiology with many relevant off-label opportunities still to be approved. Advancements in understanding microbubble physics, microbubble biophysics and the technological developments in ultrasound equipment with sensitive contrast-specific imaging methodologies have been of crucial importance for broad clinical acceptance of contrast-enhanced ultrasound imaging, turning it into a mature and successful competitor of traditional diagnostic modalities, such as contrast-enhanced MRI and CT. It is expected that for successful development of future opportunities, such as ultrasound molecular imaging and therapeutic applications using microbubbles, new creative developments in microbubble engineering and production dedicated to further optimizing microbubble performance are required, and that they cannot rely on bubble technology developed more 3 three decades ago.

*Conflict of interest disclosure*—Peter Frinking is employee of Tide Microfluidics; Ying Luan and Francois Tranquart are employees of General Elextric Healthcare.

## REFERENCES

Abdelmoneim SS, Mankad SV, Bernier M, Dhoble A, Hagen ME, Ness SC, Chandrasekaran K, Pellikka PA, Oh JK, Mulvagh SL. Microvascular function in Takotsubo cardiomyopathy with contrast echocardiography: Prospective evaluation and review of literature. J Am Soc Echocardiogr 2009a;22:1249–1255.

Abdelmoneim SS, Wijdicks EF, Lee VH, Daugherty WP, Bernier M, Oh JK, Pellikka PA, Mulvagh SL. Real-time myocardial perfusion contrast echocardiography and regional wall motion abnormalities after aneurysmal subarachnoid hemorrhage. Clinical article. J Neurosurg 2009b;111:1023–1028.

Abdelmoneim SS, Mulvagh SL. Perflutren lipid microsphere injectable suspension for cardiac ultrasound. Imaging Med 2012;4:171–191.

Albrecht T, Blomley MJ, Burns PN, Wilson S, Harvey CJ, Leen E, Claudon M, Calliada F, Correas JM, LaFortune M, Campani R, Hoffmann CW, Cosgrove DO, LeFevre F. Improved detection of hepatic metastases with pulse-inversion US during the liver-specific phase of SHU 508: A multicenter study. Radiology 2003;227:361–370.

Anna SL, Bontoux N, Stone HA. Formation of dispersions using "flow focusing" in microchannels. Appl. Phys. Lett. 2003;82:364–366.

Atchley AA, Crum LA. Acoustic cavitation and bubble dynamics. In: Suslick TS, (ed). Ultrasound: Its chemical, physical and biological effects. Weinheim, Germany: Verlagsgesellschaft; 1988. p. 1–64.

Barrera JG, Fulkerson PK, Rittgers SE, Nerem R. The nature of contrast echocardiographic "targets". Circulation 1978;58(Suppl. 11):11–233.

Becher H, Burns PN. Handbook of contrast echocardiography: Left ventricular function and myocardial perfusion. Springer Berlin Heidelberg. 2000.

Biagi E, Breschi L, Vannacci E, Masotti L. Stable and transient subharmonic emissions from isolated contrast agent microbubbles. IEEE Trans Ultrason Ferroelect Freq Contr 2007;54:480–497.

Bing C, Hong Y, Hernandez C, Rich M, Cheng B, Munaweera I, Szczepanski D, Xi Y, Bolding M, Exner A, Chopra R. Characterization of different bubble formulations for blood-brain barrier opening using a focused ultrasound system with acoustic feedback control. Sci Rep 2018;8:7986.

Blomley MJ, Albrecht T, Cosgrove DO, Patel N, Jayaram V, Butler-Barnes J, Eckersley RJ, Bauer A, Schlief R. Improved imaging of liver metastases with stimulated acoustic emission in the late phase of enhancement with the US contrast agent SH U 508A: Early experience. Radiology 1999;210:409–416.

Bokor D. Diagnostic efficacy of SonoVue. Am J Cardiol 2000;86: 19G–24G.

Bove AA, Adams DF, Hugh AE, Lynch PR. Cavitation at catheter tips. A possible cause of air embolism. Invest Radiol 1968;3:159.

Burns PN, Powers JE, Hope Simpson D, Uhlendorf V, Fritzsch T. Harmonic imaging: Principles and preliminary results. Angiology 1996;47:63–73.

Carroll BA, Turner RJ, Tickner EG, Boyle DB, Young SW. Gelatin encapsulated nitrogen microbubbles as ultrasonic contrast agents. Invest Radiol 1980;15:260–266.

Carson AR, McTiernan CF, Lavery L, Grata M, Leng X, Wang J, Chen X, Villanueva FS. Ultrasound-targeted microbubble destruction to deliver siRNA cancer therapy. Cancer Res 2012;72:6191–6199.

Castro-Hernandez E, van Hoeve W, Lohse D, Gordillo J. Microbubble generation in a co-ow device operated in a new regime. Lab Chip 2011;11:2023–2029.

Chang EH. An Introduction to Contrast-Enhanced Ultrasound for Nephrologists. Nephron 2018;138:176–185.

Chetty K, Stride E, Sennoga CA, Hajnal JV, Eckersley RJ. High-speed optical observations and simulation results of SonoVue microbubbles at low-pressure insonation. IEEE Trans Ultrason Ferroelectr Freq Control 2008;55:1333–1342.

Chin CT, Lancée C, Borsboom J, Mastik F, Frijlink ME, de Jong N, Versluis M, Lohse D. Brandaris 128: A digital 25 million frames per second camera with 128 highly sensitive frames. Rev Sci Instrum 2003;74:5026–5034.

Choi JJ, Feshitan JA, Baseri B, Wang S, Tung YS, Borden MA, Konofagou EE. Microbubble-size dependence of focused ultrasound-induced blood brain barrier opening in mice in vivo. IEEE Trans Biomed Eng 2010;57:145–154.

Church CC. The effects of an elastic solid surface layer on the radial pulsations of gas bubbles. J Acoust Soc Am 1995;97:1510–1521.

Claudon M, Dietrich CF, Choi BI, Cosgrove DO, Kudo M, Nolsoe CP, Piscaglia F, Wilson SR, Barr RG, Chammas MC, Chaubal NG, Chen MH, Clevert DA, Correas JM, Ding H, Forsberg F, Fowlkes JB, Gibson RN, Goldberg BB, Lassau N, Leen EL, Mattrey RF, Moriyasu F, Solbiati L, Weskott HP, Xu HX. Guidelines and good clinical practice recommendations for contrast enhanced Ultrasound (CEUS) in the liver -update 2012: A WFUMB-EFSUMB initiative in cooperation with representatives of AFSUMB, AIUM, ASUM, FLAUS and ICUS. Ultrasound Med Biol 2013;39:187–210.

Correas JM, Low G, Needleman L, Robbin ML, Cosgrove D, Sidhu PS, Harvey CJ, Albrecht T, Jakobsen JA, Brabrand K, Jenett M, Bates J, Claudon M, Leen E. Contrast enhanced ultrasound in the detection of liver metastases: A prospective multi-center dose testing study using a perfluorobutane microbubble contrast agent (NC100100). Eur Radiol 2011;21:1739–1746.

Dawson D, Kaul S, Peters D, Rinkevich D, Schnell G, Belcik JT, Wei K. Prognostic value of Dipyridamole stress myocardial contrast echocardiography: Comparison with single photon emission computed tomography. J Am Soc Echocardiogr 2009;22:954–960.

Deelman LE, Decleves AE, Rychak JJ, Sharma K. Targeted renal therapies through microbubbles and ultrasound. Adv Drug Deliv Rev 2010;62:1369–1377.

de Jong N, Hoff L. Ultrasound scattering properties of Albunex microspheres. Ultrasonics 1993;31:175–181.

de Jong N, Emmer M, Chin CT, Bouakaz A, Mastik F, Lohse D, Versluis M. "Compression-only" behavior of phospholipid-coated contrast bubbles. Ultrasound Med Biol 2007;33:653–656.

Dewitte H, Vanderperren K, Haers H, Stock E, Duchateau L, Hesta M, Saunders JH, De Smedt SC, Lentacker I. Theranostic mRNA-loaded microbubbles in the lymphatics of dogs: implications for drug delivery. Theranostics 2015;5:97–109.

Dietrich F, Averkiou M, Bachmann M, Barr RG, Burns PN, Calliada F, Cantisani V. How to perform contrast-enhanced Ultrasound (CEUS). Ultrasound Int Open 2018;4:E2–E15.

Doinikov AA, Bouakaz A. Review of shell models for contrast agent microbubbles. IEEE Trans Ultrason Ferroelectr Freq Control 2011;58:981–993.

Dolan MS, Riad K, El-Shafei A, Puri S, Tamirisa K, Bierig M, St Vrain J, McKinney L, Havens E, Habermehl K, Pyatt L, Kern M, Labovitz AJ. Effect of intravenous contrast for left ventricular opacification and border definition on sensitivity and specificity of dobutamine stress echocardiography compared with coronary angiography in technically difficult patients. Am Heart J 2001;142:908–915.

Dolan MS, Gala SS, Dodla S, Abdelmoneim SS, Xie F, Cloutier D, Bierig M, Mulvagh SL, Porter TR, Labovitz AJ. Safety and efficacy of commercially available ultrasound contrast agents for rest and stress echo a multicenter experience. J Am Coll Cardiol 2009;53:32–38.

Dollet B, van Hoeve W, Raven JP, Marmottant P, Versluis M. Role of the channel geometry on the bubble pinch-off in flow-focusing devices. Phys Rev Lett 2008;100 034504.

Emmer M, van Wamel A, Goertz DE, de Jong N. The onset of microbubble vibration. Ultrasound Med Biol 2007;33:941–949.

Emmer M, Vos HJ, Goertz DE, van Wamel A, Versluis M, de Jong N. Pressure-dependent attenuation and scattering of phospholipid-coated microbubbles at low acoustic pressures. Ultrasound Med Biol 2009;35:102–111.

Faez T, Goertz D, de Jong N. Characterization of Definity ultrasound contrast agent at frequency range of 5-15 MHz. Ultrasound Med Biol 2011;37:338–342.

Faez T, Emmer M, Kooiman K, Versluis M, van der Steen A, de Jong N. 20 years of ultrasound contrast agent modeling. IEEE Trans Ultrason Ferroelectr Freq Control 2013;60:7–20.

Feinstein SB, Shah PM, Bing RJ, Meerbaum S, Corday E, Chang BL, Santillan G, Fujibayashi Y. Microbubble dynamics visualized in the intact capillary circulation. J Am Coll Cardiol 1984;4:595–600.

Ferraioli G, Meloni MF. Contrast-enhanced ultrasonography of the liver using SonoVue. Ultrasonography 2018;37:25–35.
Feshitan JA, Chen CC, Kwan JJ, Borden MA. Microbubble size isolation by differential centrifugation. J Coll Interf Sci 2009;329:316–324.
Forbes MM, O'Brien WD. Development of a theoretical model describing sonoporation activity of cells exposed to ultrasound in the presence of contrast agents. J Acoustit Soc Am 2012;131:2723–2729.
Frinking P, de Jong N, Cespedes I. Scattering properties of encapsulated gas bubbles at high ultrasound pressures. J Acoust Soc Am 1999;105:1989–1996.
Frinking P, Bouakaz A, Kirkhorn J, Ten Cate FJ, de Jong N. Ultrasound contrast imaging: Current and new potential methods. Ultrasound Med Biol 2000;26:965–975.
Frinking P, Tardy I, Théraulaz M, Arditi M, Powers J, Pochon S, Tranquart F. Effects of acoustic radiation force on the binding efficiency of BR55, a VEGFR2-specific ultrasound contrast agent. Ultrasound Med Biol 2012;38:1460–1469.
Ganan-Calvo AM, Gordillo JM. Perfectly monodisperse microbubbling by capillary ow focusing. Phys Rev Lett 2001;87 274501.
Garstecki P, Gitlin I, DiLuzio W, Whitesides GM. Formation of monodisperse bubbles in a microfluidic flow-focusing device. Appl Phys Lett 2004;85:2649–2651.
Garstecki P, Stone HA, Whitesides GM. Mechanism for flow-rate controlled breakup in confined geometries: A route to monodisperse emulsions. Phys Rev Lett 2005;94 164501.
Goertz DE, de Jong N, van der Steen AFW. Attenuation and size distribution measurements of Definity and manipulated Definity populations. Ultrasound Med Biol 2007;33:1376–1388.
Gorce JM, Arditi M, Schneider M. Influence of bubble size distribution on the echogenicity of ultrasound contrast agents: A study of SonoVue. Invest Radiol 2000;35:661–671.
Gramiak R, Shah PM. Echocardiography of the aortic root. Invest Radiol 1968;3:356–366.
Gramiak R, Shah PM, Kramer DH. Ultrasound cardiography: Contrast studies in anatomy and function. Radiology 1969;92:939–948.
Greis C. Technology overview. SonoVue (Bracco, Milan). Eur Radiol 2004;8(Suppl. 14):P11–P15.
Helfield B, Chen X, Watkins SC, Villanueva FS. Biophysical insight into mechanisms of sonoporation. Proc Natl Acad Sci USA 2016;113:9983–9988.
Hernot S, Klibanov AL. Microbubbles in ultrasound-triggered drug and gene delivery. Adv Drug Deliv Rev 2008;60:1153–1166.
Hoff L, Sontum PC, Hovem JM. Oscillations of polymeric microbubbles: Effect of the encapsulating shell. J Acoust Soc Am 2000;107:2272–2280.
https://www.accessdata.fda.gov/drugsatfda_docs/label/2012/020899s015lbl.pdf.
https://www.accessdata.fda.gov/drugsatfda_docs/nda/2001/21-064_Definity.cfm.
https://www.ema.europa.eu/en/medicines/human/EPAR/luminity.
https://www.ema.europa.eu/en/medicines/human/EPAR/sonovue.
https://www.accessdata.fda.gov/drugsatfda_docs/nda/2014/203684Orig1s000TOC.cfm.
Hynynen K, McDannold N, Vykhodtseva N, Raymond S, Weissleder R, Jolesz FA, Sheikov N. Focal disruption of the blood-brain barrier due to 260-kHz ultrasound bursts: A method for molecular imaging and targeted drug delivery. J Neurosurg 2006;105:445–454.
Hyvelin JM, Gaud E, Costa M, Helbert A, Bussat P, Bettinger T, Frinking P. Characteristics and echogenicity of clinical ultrasound contrast agents: An in vitro and in vivo comparison study. J Ultrasound Med 2017;36:941–953.
Jackson A, Castle JW, Smith A, Kalli CK. Optison albumin microspheres in ultrasound assisted gene therapy and drug delivery. In: Otagiri M, Chuang V, (eds). Albumin in medicine: Pathological and clinical applications. Singapore: Springer; 2016.
Jo P, Jang H, Burns P, Burak K, Kim T, Wilson S. Integration of contrast-enhanced US into a multimodality approach to imaging of nodules in a cirrhotic liver: How to do it. Radiology 2017;282.
Jung EM, Clevert DA, Rupp N. Contrast-Enhanced Ultrasound with® Optison in Percutaneous Thermoablation of Liver Tumors. Fortschr Röntgenstr 2003;175:1403–1412.
Karshafian R, Bevan PD, Williams R, Samac S, Burns PN. Sonoporation by ultrasound-activated microbubble contrast agents: Effect of acoustic exposure parameters on cell membrane permeability and cell viability. Ultrasound Med Biol 2009;35:847–860.
Kasprzak JD, Ten Cate FJ. New ultrasound contrast agents for left ventricular and myocardial opacification. Herz 1998;23:474–482.
Katiyar A, Sarkar K. Excitation threshold for subharmonic generation from contrast microbubbles. J Acoust Soc Am 2011;130:3137–3147.
Kaya M, Feingold S, Hettiarachchi K, Lee AP, Dayton PA. Acoustic responses of monodisperse lipid-encapsulated microbubble contrast agents produced by flow focusing. Bubble Sci Eng Technol 2010;2:33–40.
Kerber RE, Kioschos JM, Lauer RM. Use of an ultrasonic contrast method in the diagnosis of valvular regurgitation and intracardiac shunts. Am J Cardiol 1974;34:722–727.
Klibanov AL. Microbubble contrast agents: Targeted ultrasound imaging and ultrasound-assisted drug-delivery applications. Invest Radiol 2006;41:354–362.
Kok MP, Segers T, Versluis M. Bubble sorting in pinched microchannels for ultrasound contrast agent enrichment. Lab Chip 2015;15:3716–3722.
Konofagou EE, Tung YS, Choi J, Deffieux T, Baseri B, Vlachos F. Ultrasound-induced blood-brain barrier opening. Curr Pharm Biotechnol 2012;13:1332–1345.
Kremkau FW, Gramiak R, Carstensen EL, Shah PM, Kramer DH. Ultrasonic detection of cavitation at catheter tips. Am J Roentgenol 1968;3:159.
Kremkau FW, Gramiak R, Carstensen EL, Shah PM, Kramer DH. Ultrasonic detection of cavitation at catheter tips. Am J Roentgenol 1970;110:177–183.
Kudo M. Defect reperfusion imaging with Sonazoid: A breakthrough in hepatocellular carcinoma. Liver Cancer 2016;5:1–7.
Leighton TG. The acoustic bubble. San Diego, CA: Academic Press; 1994.
Li P, Hoppmann S, Du P, Li H, Evans P, Moestue S, Yu W, Dong F, Liu H, Liu L. Pharmacokinetics of perfluorobutane after intravenous bolus injection of Sonazoid in healthy Chinese volunteers. Ultrasound Med Biol 2017;43:1031–1039.
Lu MD, Yu XL, Li AH, Jiang TA, Chen MH, Zhao BZ, Zhou XD, Wang JR. Comparison of contrast enhanced ultrasound and contrast enhanced CT or MRI in monitoring percutaneous thermal ablation procedure in patients with hepatocellular carcinoma: A multi-center study in China. Ultrasound Med Biol 2007;33:1736–1749.
Marmottant P, VanderMeer S, Emmer M, Versluis M, de Jong N, Hilgenfeldtb S, Lohse D. A model for large amplitude oscillations of coated bubbles accounting for buckling and rupture. J Acoust Soc Am 2005;118:3499–3505.
Marmottant P, Bouakaz A, de Jong N, Quilliet C. Buckling resistance of solid shell bubbles under ultrasound. J Acoust Soc Am 2011;129:1231–1239.
McCarville MB, Kaste SC, Hoffer FA, Khan RB, Walton RC, Alpert BS, Furman WL, Li C, Xiong X. Contrast enhanced sonography of malignant pediatric abdominal and pelvic solid tumors: Preliminary safety and feasibility data. Pediatr Radiol 2012;42:824–833.
Medwin H. Counting bubbles acoustically: a review. Ultrasonics 1977;15:7–13.
Meloni MF, Bertolotto M, Alberzoni C, Lazzaroni S, Filice C, Livraghi T, Ferraioli G. Follow-up after percutaneous radiofrequency ablation of renal cell carcinoma: Contrast-enhanced sonography versus contrast-enhanced CT or MRI. AJR Am J Roentgenol 2008;191:1233–1238.
Meltzer R, Tickner G, Sahines T, Popp RL. The source of ultrasonic contrast effect. J Clin Ultrasound 1980;8:121.
Contrast echocardiography. In: Meltzer RS, Roelandt J, (eds). Contrast echocardiography. The Hague/Boston/London: Martinus Nijhoff Publishers; 1982.
Main ML, Goldman JH, Rayburn PA. Thinking outside the "box"-The ultrasound contrast controversy. J Am Coll Cardiology 2007;50:2434–2437.
Minnaert M. On musical air-bubbles and the sound of running water. Philosophical Magazine 1933;16:235–248.

Moir S, Haluska BA, Jenkins C, Fathi R, Marwick TH. Incremental benefit of myocardial contrast to combined dipyridamole-exercise stress echocardiography for the assessment of coronary artery disease. Circulation 2004;110:1108–1113.

Molina CA, Barreto AD, Tsivgoulis G, Sierzenski P, Malkoff MD, Rubiera M, Gonzales N, Mikulik R, Pate G, Ostrem J, Singleton W, Manvelian G, Unger EC, Grotta JC, Schellinger PD, Alexandrov AV. Transcranial ultrasound in clinical sonothrombolysis (TUCSON) trial. Ann Neurol 2009;66:28–38.

Morgan KE, Allen JS, Dayton PA, Chomas JE, Klibanov AL, Ferrara KW. Experimental and theoretical evaluation of microbubble behavior: Effect of transmitted phase and bubble size. IEEE Trans Ultrason Ferroelect Freq Contr 2000;47:1494–1509.

Moriyasu F, Itoh K. Efficacy of perflubutane microbubble-enhanced ultrasound in the characterization and detection of focal liver lesions: Phase 3 multicenter clinical trial. Am J Roentgenol 2009; 193:86–95.

Mulvagh SL, Rakowski H, Vannan MA, Abdelmoneim SS, Becher H, Bierig SM, Burns PN, Castello R, Coon PD, Hagen ME, Jollis JG, Kimball TR, Kitzman DW, Kronzon I, Labovitz AJ, Lang RM, Mathew J, Moir WS, Nagueh SF, Pearlman AS, Perez JE, Porter TR, Rosenbloom J, Strachan GM, Thanigaraj S, Wei K, Woo A, Yu EH, Zoghbi WA. American Society of Echocardiography consensus statement on the clinical applications of ultrasonic contrast agents in echocardiography. J Am Soc Echocardiogr 2008;21:1179–1201.

Mulvana H, Browning RJ, Luan Y, de Jong N, Tang MX, Eckersley RJ, Stride E. Characterization of contrast agent microbubbles for ultrasound imaging and therapy research. IEEE Trans Ultrason Ferroelect Freq Contr 2017;63:232–251.

Ntoulia A, Back SJ, Poznick L, Morgan T, Kerwood J, Christopher EJ, Bellarh RD, Reid JR, Jaramillo D, Canning DA, Darge K. Contrast-enhanced voiding urosonography (ceVUS) with the intravesical administration of the ultrasound contrast agent Optison for vesicoureteral reflux detection in children: A prospective clinical trial. Pediatr Radiol 2018;48:216–226.

Ophir J, Parker KJ. Contrast agents in diagnostic ultrasound. Ultrasound Med Biol 1989;15:319–333.

Overvelde M, Garbin V, Sijl J, Dollet B, de Jong N, Lohse D, Versluis M. Nonlinear shell behavior of phospholipid-coated microbubbles. Ultrasound Med Biol 2010;36:2080–2092.

Overvelde M, Garbin V, Dollet B, de Jong N, Lohse D, Versluis M. Dynamics of coated microbubbles adherent to a wall. Ultrasound Med Biol 2011;37:1500–1508.

Paefgen V, Doleschel D, Kiessling F. Evolution of contrast agents for ultrasound imaging and ultrasound-mediated drug delivery. Front Pharmacol 2015;197:1–16.

Paul S, Katiyar A, Sarkar K, Chatterjee D, Shi WT, Forsberg F. Material characterization of the encapsulation of an ultrasound contrast microbubble and its subharmonic response: Strain-softening interfacial elasticity model. J Acoust Soc Am 2010;127:3846–3857.

Plana JC, Mikati IA, Dokainish H, Lakkis N, Abukhalil J, Davis R, Hetzell BC, Zoghbi WA. A randomized cross-over study for evaluation of the effect of image optimization with contrast on the diagnostic accuracy of dobutamine echocardiography in coronary artery disease: The OPTIMIZE trial. JACC Cardiovasc Imaging 2008;1:145–152.

Pochon S, Tardy I, Bussat P, Bettinger T, Brochot J, von Wronski M, Passantino L, Schneider M. BR55: A lipopeptide-based VEGFR2-targeted ultrasound contrast agent for molecular imaging of angiogenesis. Invest Radiol 2010;45:89–95.

Podell S, Burrascano C, Gaal M, Golec B, Maniquis J, Mehlhaff P. Physical and biochemical stability of Optison, an injectable ultrasound contrast agent. Biotechnol Appl Biochem 1999;30:213–223.

Porter TM, Smith DAB, Holland CK. Acoustic techniques for assessing the Optison destruction threshold. J Ultrasound Med 2006;25:1519–1529.

Porter TR, Abdelmoneim SS, Belcik JT, McCulloch ML, Mulvagh SL, Olson JJ, Porcelli C, Tsutsui JM, Wei K. Guidelines for the cardiac sonographer in the performance of contrast echocardiography: A focused update from the American Society of Echocardiography. J Am Soc Echocardiogr 2014;27:797–810.

Porter TR, Mulvagh SL, Abdelmoneim SS, Becher H, Belcik JT, Bierig M, Choy J, Gaibazzi N, Gillam LD, Janardhanan R, Kutty S, Leong-Poi H, Lindner JR, Main ML, Mathias W, Jr, Park MM, Senior R, Villanueva F. Clinical applications of ultrasonic enhancing agents in echocardiography: 2018 American Society of Echocardiography guidelines update. J Am Soc Echocardiogr 2018;31:241–274.

Quaia E. Classification and safety of microbubble-based contrast agents. Contrast media in ultrasonography: Basic principles and clinical applications. Berlin, Heidelberg: Springer Berlin Heidelberg; 2005. p. 3–14.

Quaia E, Gennari AG, Angileri R, Cova MA. Bolus versus continuous infusion of microbubble contrast agent for liver ultrasound by using an automatic power injector in humans: A pilot study. J Clin Ultrasound 2016;44:136–142.

Rafter P, Phillips P, Vannan MA. Imaging technologies and techniques. Cardiol Clin 2004;22:181–197.

Reid CL, Kawanishi DT, McKay CR. Accuracy of evaluation of the presence and severity of aortic and mitral regurgitation by contrast 2-dimensional echocardiography. Am J Cardiol 1983; 52:519–524.

Roelandt J. Contrast echocardiography. Ultrasound Med Biol 1982; 8:471.

Roovers S, Segers T, Lajoinie G, Deprez J, Versluis M, De Smedt SC, Lentacker I. The role of ultrasound-driven microbubble dynamics in drug delivery: From microbubble fundamentals to clinical translation. Langmuir 2019;35:10173–10191.

Sarkar K, Shi WT, Chatterjee D, Forsberg F. Characterization of ultrasound contrast microbubbles using in vitro experiments and viscous and viscoelastic interface models for encapsulation. J Acoust Soc Am 2005;118:539–550.

Schneider M, Arditi M, Barrau MB, Brochot J, Broillet A, Ventrone R, Yan F. BR1: A new ultrasonographic contrast agent based on sulfur hexafluoride-filled microbubbles. Invest Radiol 1995;30:451–457.

Schneider M, Broillet A, Bussat P, Giessinger N, Puginier J, Ventrone R, Yan F. Gray-scale liver enhancement in VX2 tumor-bearing rabbits using BR14, a new ultrasonographic contrast agent. Invest Radiol 1997;32:410–417.

Schneider M. Bubbles in echocardiography: Climbing the learning curve. Eur Heart J Suppl 2002;4(Suppl. C):C3–C7.

Schneider M, Anantharam B, Arditi M, Bokor D, Broillet A, Bussat P, Fouillet X, Frinking P, Tardy I, Terrettaz J, Senior R, Tranquart F. BR38, a new ultrasound blood pool agent. Invest Radiol 2011; 46:486–494.

Schuchman H, Feigenbaum H, Dillon JC, Chang S. Intracavitary echoes in patients with mitral prosthetic valves. J Clin Ultrasound 1975;3:107.

Segers T, de Jong N, Lohse D, Versluis M. In Microbubbles for medical applications. London: Royal Society of Chemistry 2014; pp. 81–101.

Segers T, Versluis M. Acoustic bubble sorting for ultrasound contrast agent enrichment. Lab Chip 2014;14:1705–1714.

Segers T, de Jong N, Versluis M. Uniform scattering and attenuation of acoustically sorted ultrasound contrast agents: Modeling and experiments. J Acoust Soc Am 2016a;140:2506–2517.

Segers T, de Rond L, de Jong N, Borden M, Versluis M. Stability of monodisperse phospholipid-coated microbubbles formed by flow-focusing at high production rates. Langmuir 2016b;32:3937–3944.

Segers T, Lohse D, Versluis M, Frinking P. Universal equations for the coalescence probability and long-term size stability of phospholipid-coated monodisperse microbubbles formed by ow-focusing. Langmuir 2017;33:10329–10339.

Segers T, Gaud E, Versluis M, Frinking P. High-precision acoustic measurements of the nonlinear dilatational elasticity of phospholipid coated monodisperse microbubbles. Soft Matter 2018a;14:9550–9561.

Segers T, Kruizinga P, Kok M, Lajoinie G, de Jong N, Versluis M. Monodisperse versus polydisperse ultrasound contrast agents: Nonlinear response, sensitivity, and deep tissue imaging potential. Ultrasound Med Biol 2018b;44:1482–1492.

Segers T, Lassus A, Bussat P, Gaud E, Frinking P. Improved coalescence stability of monodisperse phospholipid-coated microbubbles formed by flow-focusing at elevated temperatures. Lab Chip 2019;19:158–167.

Senior R, Becher H, Monaghan M, Agati L, Zamorano J, Vanoverschelde JL, Nihoyannopoulos P, Edvardsen T, Lancellotti P. Clinical practice of contrast echocardiography: Recommendation by the European Association of Cardiovascular Imaging (EACVI) 2017. Eur Heart J Cardiovasc Imaging 2017;18 1205a−1205af.

Shimazu K, Ito T, Uji K, Miyake T, Aono T, Motomura K, Naoi Y, Shimomura A, Shimoda M, Kagara N, Kim SJ, Noguchi S. Identification of sentinel lymph nodes by contrast-enhanced ultrasonography with Sonazoid in patients with breast cancer: A feasibility study in three hospitals. Cancer Med 2017;6:1915–1922.

Sidhu PS, Cantisani V, Deganello A, Dietrich CF, Duran C, Franke D, Harkanyi Z, Kosiak W, Miele V, Ntoulia A, Piskunowicz M, Sellars ME, Gilja OH. Role of contrast-enhanced ultrasound (CEUS) in paediatric practice: An EFSUMB position statement. Ultraschall Med 2017;38:33–43.

Sidhu PS, Cantisani V, Dietrich CF, Gilja OH, Saftoiu A, Bartels E, Bertolotto M, Calliada F, Clevert DA, Cosgrove D, Deganello A, D'Onofrio M, Drudi FM, Freeman S, Harvey C, Jenssen C, Jung EM, Klauser AS, Lassau N, Meloni MF, Leen E, Nicolau C, Nolsoe C, Piscaglia F, Prada F, Prosch H, Radzina M, Savelli L, Weskott HP, Wijkstra H. The EFSUMB guidelines and recommendations for the clinical practice of contrast-enhanced ultrasound (CEUS) in non-hepatic applications: Update 2017 (long version). Ultraschall Med 2018;39:e2–e44.

Simpson DH, Chin CT, Burns PN. Pulse inversion Doppler: A new method for detecting nonlinear echoes from microbubble contrast agents. IEEE Trans Ultrason Ferroelect Freq Contr 1999;46:372–382.

Smeenge M, Tranquart F, Mannaerts CK, de Reijke TM, van de Vijver MJ, Laguna MP, Pochon S, de la Rosette JJMCH, Wijkstra H. First-in-human ultrasound molecular imaging with a VEGFR2-specific ultrasound molecular contrast agent (BR55) in prostate cancer: A safety and feasibility pilot study. Invest Radiol 2017;52:419–427.

Snipstad S, Berg S, Morch Y, Bjorkoy A, Sulheim E, Hansen R, Grimstad I, van Wamel A, Maaland AF, Torp SH, De Lange Davies C. Ultrasound improves the delivery and therapeutic effect of nanoparticle-stabilized microbubbles in breast cancer xenografts. Ultrasound Med Biol 2017;43:2651–2669.

Sontum PC, Østensen J, Dyrstad K, Hoff L. Acoustic properties of NC100100 and their relationship with the microsphere size distribution. Invest Radiol 1999;34:268–275.

Sontum PC. Physicochemical characteristics of Sonazoid, a new contrast for ultrasound imaging. Ultrasound Med Biol 2008;34:824–833.

Streeter JE, Gessner R, Miles I, Dayton PA. Improving sensitivity in ultrasound molecular imaging by tailoring contrast agent size distribution: in vivo studies. Mol Imaging 2010;9:87–95.

Stride E, Saffari N. Microbubble ultrasound contrast agents: A review. Proc Inst Mech Eng H 2003;217:429–476.

Stride E. The influence of surface adsorption on microbubble dynamics. Philos Trans A Math Phys Eng Sci 2008;366:2103–2115.

Stride E, Edirisinghe M. Novel preparation techniques for controlling microbubble uniformity: A comparison. Med Biol Eng Comput 2009;47:883–892.

Talu E, Hettiarachchi K, Zhao S, Powell RL, Lee AP, Longo ML, Dayton PA. Tailoring the size distribution of ultrasound contrast agents: Possible method for improving sensitivity in molecular imaging. Mol Imaging 2007;6:384–392.

Tardy I, Pochon S, Theraulaz M, Emmel P, Passantino L, Tranquart F, Schneider M. Ultrasound molecular imaging of VEGFR2 in a rat prostate tumor model using BR55. Invest Radiol 2010;45:573–578.

Tranquart F, Arditi M, Bettinger T, Frinking P, Hyvelin JM, Nunn A, Pochon S, Tardy I. Ultrasound contrast agents for ultrasound molecular imaging. Z Gastroenterol 2014;52:1268–1276.

Tsiglifis K, Pelekasis NA. Nonlinear radial oscillations of encapsulated microbubbles subject to ultrasound: The effect of membrane constitutive law. J Acoust Soc Am 2008;123:4059–4070.

Tsutsui JM, Xie F, Porter RT. The use of microbubbles to target drug delivery. Cardiovasc Ultrasound 2004;2:23.

Tsutsui JM, Elhendy A, Xie F, O'Leary EL, McGrain AC, Porter TR. Safety of dobutamine stress real-time myocardial contrast echocardiography. J Am Coll Cardiol 2005;45:1235–1242.

Tu J, Guan J, Qiu Y, Matula TJ. Estimating the shell parameters of SonoVue microbubbles using light scattering. J Acoust Soc Am 2009;126:2954–2962.

Unger E, Shen D, Fritz T, Kulik B, Lund P, Wu GL, Yellowhair D, Ramaswami R, Matsunage T. Gas-filled lipid bilayers as ultrasound contrast agents. Invest Radiol 1994;29:134–136.

Valdes-Cruz LM, Sahn DJ. Ultrasonic contrast studies for the detection of cardiac shunts. J Am Coll Cardiol 1984;3:978–985.

VanderMeer SM, Versluis M, Lohse D, Chin CT, Bouakaz A, de Jong N. The resonance frequency of SonoVue™ as observed by high-speed optical imaging. Proceedings of the IEEE Ultrasonics Symposium 2004;1:343–345.

Van Rooij T, Skachkov I, Beekers I, Lattwein KR, Voorneveld JD, Kokhuis TJ, Bera D, Luan Y, van der Steen AF, de Jong N, Kooiman K. Viability of endothelial cells after ultrasound-mediated sonoporation: Influence of targeting, oscillation, and displacement of microbubbles. J Control Release 2016;238:197–211.

Wang TY, Choe JW, Pu K, Devulapally R, Bachawal S, Machtaler S, Chowdhury SM, Luong R, Tian L, Khuri-Yakub B, Rao J, Paulmurugan R, Willmann JK. Ultrasound-guided delivery of microRNA loaded nanoparticles into cancer. J Control Release 2015;203:99–108.

Watanabe R, Matsumura M, Munemasa T, Fujimaki M, Suematsu M. Mechanism of hepatic parenchyma-specific contrast of microbubble-based contrast agent for ultrasonography: Microscopic studies in rat liver. Invest Radiol 2007;42:643–651.

Wei K, Jayaweer AR, Firoozan S, Linka A, Skyba DM, Kaul S. Quantification of myocardial blood flow with ultrasound-induced destruction of microbubbles administered as a constant venous infusion. Circulation 1998;97:473–483.

Willmann JK, Bonomo L, Testa AC, Rinaldi P, Rindi G, Valluru KS, Petrone G, Martini M, Lutz AM, Gambhir SS. Ultrasound molecular imaging with BR55 in patients with breast and ovarian lesions: First-in-human results. J Clin Oncol 2017;35:2133–2140.

Yanagisawa K, Moriyasu F, Miyahara T, Yuki M, Iijima H. Phagocytosis of ultrasound contrast agent microbubbles by Kupffer cells. Ultrasound Med Biol 2007;33:318–325.

Zhai HY, Liang P, Yu J, Cao F, Kuang M, Liu FY, Liu FY, Zhu XY. Comparison of Sonazoid and Sonovue in the diagnosis of focal liver lesions: A preliminary study. J Ultrasound Med 2019;38:2417–2425.

Zhao H, O'Quinn R, Ambrose M, Jagasia D, Ky B, Wald J, Ferrari VA, Kirkpatrick JN, Han Y. Contrast-enhanced echocardiography has the greatest impact in patients with reduced ejection fractions. J Am Soc Echocardiogr 2017;31:289–296.

Ziskin MC, Bonakdarpour A, Weinstein DP, Lynch PR. Contrast agents for diagnostic ultrasound. Invest Radiol 1972;7:500–505.